Resolving the Hanbury Brown–Twiss Puzzle in Relativistic Heavy Ion Collisions

Scott Pratt

Department of Physics and Astronomy, Michigan State University, East Lansing, Michigan 48824, USA

(Received 20 November 2008; revised manuscript received 8 April 2009; published 8 June 2009)

Two particle correlation data from the BNL Relativistic Heavy Ion Collider have provided detailed femtoscopic information describing pion emission. In contrast with the success of hydrodynamics in reproducing other classes of observables, these data had avoided description with hydrodynamic-based approaches. This failure has inspired the term ''HBT puzzle,'' where HBT refers to femtoscopic studies which were originally based on Hanbury Brown–Twiss interferometry. Here, the puzzle is shown to originate not from a single shortcoming of hydrodynamic models, but the combination of several effects: mainly prethermalized acceleration, using a stiffer equation of state, and adding viscosity.

DOI: 10.1103/PhysRevLett.102.232301 PACS numbers: 25.75.Gz, 25.75.Ld

Experiments at the BNL Relativistic Heavy Ion Collider (RHIC) have revealed a new state of matter, the strongly interacting quark gluon plasma (QGP), which appears to have perhaps the lowest ratio of viscosity to entropy of any measured substance [1,2]. This conclusion is based on comparisons of hydrodynamic models with experimental spectra and large angle correlations that reveal strong radial and elliptic collective flow, i.e., flow relative to the original beam axis. The most sophisticated hydrodynamic approaches also employ microscopic simulations to model the decoupling stage. Whereas spectra and large angle correlations are consistent with ideal hydrodynamics [3,4], these same models have poorly reproduced correlations at small-relative momentum [4–6]. These correlations are related to the spatial and temporal properties of pion emission [7], and are often referred to as Hanbury Brown–Twiss (HBT) measurements after similar measurements with light [8]. It appears that hydrodynamic models underestimate the explosiveness of the collision, or equivalently overestimate the duration of the emission process. In contrast, some purely microscopic approaches have been more successful in reproducing the data [9–12]. Unlike the hydrodynamic models, which employed first-order phase transitions, the effective equations of state for the microscopic approaches are extremely stiff, leading to more explosive collisions. In short, the HBT puzzle involves finding whether one can reproduce femtoscopic observations with hydrodynamic models without employing any particularly strange assumptions, such as equations of state that are inconsistent with lattice calculations, or arbitrary breakup criteria that are inconsistent with known properties of binary hadronic reaction. In this Letter, we show this can be accomplished if three improvements are incorporated into hydrodynamic models: accounting for the buildup of collective flow in the first instants of the collision before thermalization is attained, using a stiffer equation of state, and including viscosity. The hydrodynamic model used here, which can be seen in more detail in [13], is the first to incorporate all these features and investigate the cumulative effects, while also being coupled to a detailed microscopic simulation for the breakup stage. The individual effects have all been discussed or studied individually. For instance, Broniowski *et al.* were able to largely reproduce the same effects without viscosity, but only after using a compact Gaussian initial profile and a simplified freeze-out prescription, both of which are difficult to justify [14].

The Koonin equation [15] relates the experimentally measured correlation function to the outgoing phase-space density,

$$C(\mathbf{P},\mathbf{q}) = \int d^3r S(\mathbf{P},r)|\phi(\mathbf{q},\mathbf{r})|^2. \quad (1)$$

Here, P and q are the total and relative momentum. The source function $S(\mathbf{P},\mathbf{r})$ describes the probability for two particles with identical momenta $\mathbf{k} = \mathbf{P}/2$, to be separated by $\mathbf{r}$ in their asymptotic state if the relative interaction between the particles were to be ignored. Since S refers to the outgoing phase-space cloud for a specific $\mathbf{k}$, quoted sizes tend to be significantly smaller than the overall source volume. Any dynamical model, whether based on hydrodynamics or microscopic degrees of freedom, provides a list of positions and times from which particles of specific $\mathbf{k}$ are emitted, and can then be used to generate the source function. For the purposes of this Letter we will only consider parameters extracted by fitting to correlations that arise from a Gaussian source,

$$S(\mathbf{P},\mathbf{r}) \sim \exp\left\{-\frac{x^2}{4R_{\rm out}^2} - \frac{y^2}{4R_{\rm side}^2} - \frac{z^2}{4R_{\rm long}^2}\right\}. \quad (2)$$

$R_{\rm long}$ describes the longitudinal size along the beam axis, $R_{\rm out}$ is the outward dimension parallel to $\mathbf{k}$, and $R_{\rm side}$ describes the extent along the sideward dimension perpendicular to both the beam axis and $\mathbf{k}$. Each of these dimensions can be a function of the transverse momentum k_t and the longitudinal rapidity of the pair. Here, we consider only central collisions and the k_t dependence of the Gaussian dimensions.

Figure 1 shows experimentally determined radius parameters from 100A GeV Au on 100A GeV Au collisions

 © 2009 The American Physical Society

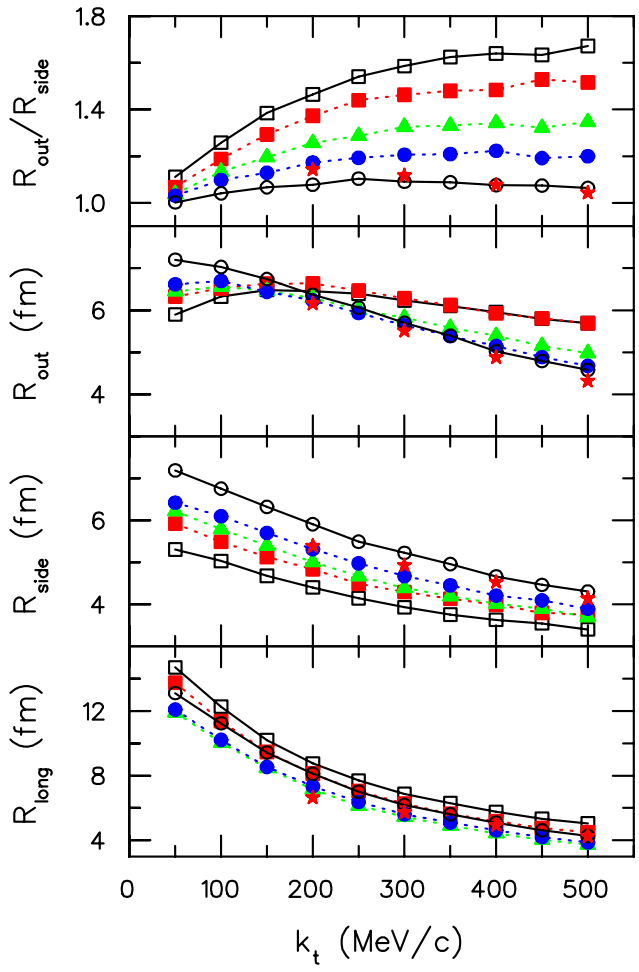

FIG. 1 (color online). Gaussian radii in three directions: R_{out}, R_{side}, and R_{long}. Data from STAR (red stars) [16] are poorly fit by a model with a first-order phase transition, no prethermal flow, and no viscosity (open black squares and solid line). Data are better reproduced after including all the features (open circles, solid black line). The incremental improvements (open colored symbols and dashed lines) are of similar strength: initial flow (red squares), stiffer equation of state (green triangles), viscosity (blue circles). Incorporating a more compact initial profile represents the final feature.

at RHIC [16]. For comparison, source sizes were generated from a hydrodynamic model coupled to a cascade code. The cascade microscopically simulates the final stages of the collision and breakup where local kinetic equilibrium is lost and hydrodynamics is unjustified. The times and positions of last collisions for particles of a specific $\mathbf{k}$ were used to calculate the source function, from which correlation functions were generated via Eq. (1). These were then fit to correlations from Gaussian sources to extract radii. For all the calculations shown here, the full wave function, including Coulomb and strong interactions, was employed, with the fitting performed via the Bowler-Sinyukov procedure used by the experiments [17,18].

As a benchmark, the first calculation (open squares in Fig. 1) was parametrized similarly to previous hydrodynamic calculations, and failed in a similar manner. Transverse expansion was delayed until 1 fm/c after the initial collision. A strong first-order phase transition, which is inconsistent with lattice gauge theory, was employed, and the viscosities were set to zero. The $R_{\mathrm{out}}/R_{\mathrm{side}}$ ratio is too large by $\sim$50% and overstates R_{long} by $\sim$25%. The second calculation (filled squares in Fig. 1) accounts for prethermal acceleration by beginning the expansion 0.1 fm/c after the initial collision, roughly the amount of time required for the Lorentz contracted nuclei to traverse one another. The importance of prethermalized acceleration for HBT studies has been emphasized in several studies during the past few years [10,14,19], and has been investigated in much greater detail in regards to other observables [20–22]. As was shown in [23], flow during the first 1 fm/c is approximately universal for any system with a traceless energy tensor, including partonic and field based pictures, independent of thermalization. Since the transverse expansion starts earlier, the longitudinal size is smaller at breakup, more in line with data. The $R_{\mathrm{out}}/R_{\mathrm{side}}$ ratios also drop, moving modestly toward the data.

The second improvement to be considered is to use a stiffer equation of state. Early studies used an equation of state with a first-order phase transition with a large latent heat [4–6]. Such soft equations of state have constant temperature and pressure for energy densities between ϵ_h and $\epsilon_h + L$, where ϵ_h is the maximum density of the hadronic phase. Here, ϵ_h corresponds to a hadronic gas with a temperature of $T_c = 170$ MeV, and L is the latent heat. In contrast, lattice QCD now suggests a crossover transition where the pressure rises continuously with energy density. There indeed exists a soft region, but the speed of sound, $c_s^2 = dP/d\epsilon$, never falls below 0.1 and the width of the soft region is somewhat lower than the latent heat L assumed in the previous studies. The benchmark calculation, displayed in the upper panel, assumed a first-order transition with a large latent heat $L = 1.6$ GeV/fm^3 with a lower bound to the mixed phase at $\epsilon_h \approx 500$ MeV/fm^3. For a first-order phase transition the lower pressure results in less explosivity and in longer lifetimes and extended values of the outward dimensions of the phase-space cloud [24,25]. This was not observed. The third calculation (filled triangles in Fig. 1) assumed a soft region of half the width in energy density, and with a speed of sound of $c_s^2 = 0.1$, rather than zero for a first-order transition. Once above the soft region, both calculations assumed a stiffening with the speed of sound $c_s^2 = 0.3$. One can consult Ref. [26] for a more sophisticated attempt at parametrizing lattice equations of state. As expected, the stiffer equation of state led to less extended outward dimensions, which lowers the $R_{\mathrm{out}}/R_{\mathrm{side}}$ ratio. In Fig. 1 the $R_{\mathrm{out}}/R_{\mathrm{side}}$ ratio again moved toward the data.

Shear viscosity is also known to increase the explosiveness of the collision [13,27,28]. This can be understood by considering viscous corrections to the stress-energy tensor. At early times the velocity gradient is largely longitudinal,

which affects the stress-energy tensor by strengthening the transverse pressure, T_{xx} and T_{yy}, and decreasing the longitudinal pressure. In the Navier-Stokes equation,

$$\Delta T_{xx} = \frac{2\eta}{3\tau}, \qquad \Delta T_{zz} = -\frac{4\eta}{3\tau}, \tag{3}$$

where η is the shear viscosity and the velocity gradient for early times is $dv_z/dz = 1/\tau$. After the first few fm/c, the transverse acceleration is determined by T_{xx} and T_{yy}. As originally demonstrated in [28], and shown here in the lower panel of Fig. 1, the $R_{\rm out}/R_{\rm side}$ ratio can be lowered by $\sim$10% with realistic shear viscosities. Analyses of elliptic flow have pointed to a small shear viscosity [28], perhaps approaching the KSS limit [29], $\eta_{\rm KSS} = s/4\pi$, where s is the entropy density. The neglect of prethermalized flow in these calculations might have led to underestimates of the viscosity, but nonetheless, it is expected that η is not much greater than the KSS bound. Below T_c, collisions are binary and the cascade prescription naturally accounts for viscous effects. Bulk viscosity is expected to be important near T_c due to the inability of the system to maintain equilibrated chiral fields near T_c [30,31]. The impact of adding viscosity, as shown in Fig. 1 (filled circles), is mainly driven by shear.

There is consensus that the three improvements discussed thus far should be incorporated into models, though the magnitude of the effects is open to debate. A fourth change, that is somewhat more contentious, involves changing the initial energy density profile. The shape employed thus far is based on the wounded nucleon model [32], but more compact profiles have been shown to increase the explosiveness and lower the $R_{\rm out}/R_{\rm side}$ ratio [13,14]. As an example, calculations using more compact profile based on [33] are shown in Fig. 1 (open circles). The $R_{\rm out}/R_{\rm side}$ ratio again falls, though the overall fit to data is not improved. The model used here assumed boost-invariant accelerationless flow along the beam axis, but this approximation is only approximate, and is expected to cause errors of a few percent in HBT radii, most likely leading to a lowering of $R_{\rm long}$ by a few percent [34]. Another effect not considered here concerns the interaction of the outgoing pions with a mean field from the remaining matter [35]. Given the breakup densities of $\lesssim 0.1$ per fm^3, fields and the related distortions are expected be only at the few percent level [36].

The second puzzling aspect of HBT analyses concerns fits with bast-wave models, which are based on a picture of thermal emission from a collectively expanding source, parametrized by a breakup temperature T, an outer radius R, a breakup time τ, a linearly rising transverse collective velocity with a maximum $v_{\rm max}$, and an emission duration $\Delta\tau$. These fits revealed outer radii near 12 fm, with emission confined to within a few fm/c of $\tau = 10$ fm/c [37,38]. Even though these radii are noticeably larger than the HBT radii, which reflect only a subset of the overall size, the parameters suggest an unphysically high breakup density corresponding to mean free paths of 1–2 fm. Figure 2 shows the outward coordinate x and the time τ at which emission occurred for the final model in Fig. 1, and are similar to what was seen in [12]. Points are shown only for particles emitted with momentum $p_x = 300$ MeV/c. Emission comes mostly from within a few fm of the surface, and there exists a modestly positive correlation between x and t, as the average x for the emission points moves outward at approximately a tenth the speed of light. A positive correlation prevents those particles produced at later times from being strongly separated from those emitted earlier, which leads to smaller outward sizes of the outgoing phase-space packet. Other physics elements of the breakup are also missing from blast wave pictures, such as the differential cooling and collective flow of protons and pions once they lose equilibrium [39]. This emphasizes the importance of using realistic dynamical models to compare to femtoscopic data and underscores the limits of parametric fits.

Shear, early flow and applying a stiffer equation of state all increase the explosivity and lead to more radial flow. The relative spectral shapes of heavy (protons) and light (pions) is understood to be a good indicator of radial collective flow, since heavier particles are more strongly influenced by flow. Bulk viscosity had little effect on the HBT radii but did soften the collective flow. The result is a reasonably good match to PHENIX spectral shapes displayed in Fig. 3. Baryon yields were overestimated which required a rescaling of the proton spectra by 0.7, perhaps due to the lack of baryon annihilation processes in the cascade. Unfortunately, bulk viscosity is theoretically uncertain. For the calculations shown here, the bulk viscosity was set to zero in the QGP and hadronic phases. Rather arbitrarily, it was set to behave linearly as a function of the

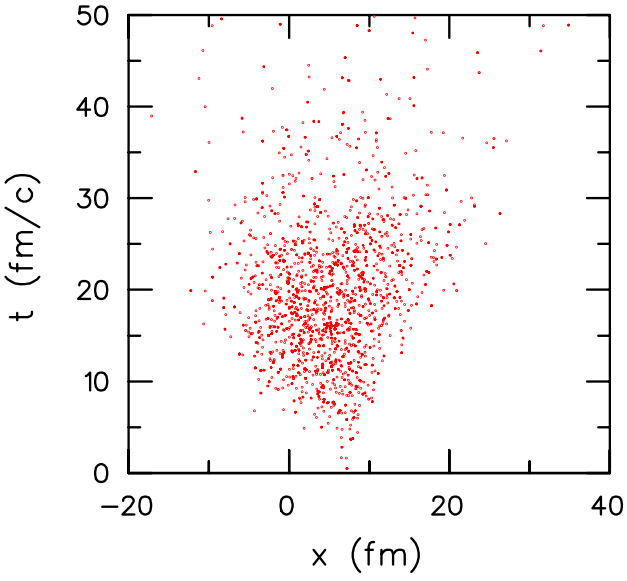

FIG. 2 (color online). Final emission positions and times for particles with transverse momentum of 300 MeV/c along the x (outward) axis. Emission is surface dominated and has a modestly positive correlation between x and t.

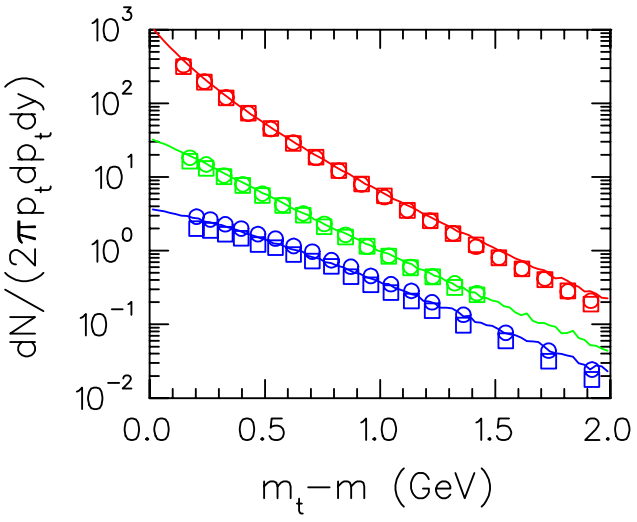

FIG. 3 (color online). Model spectra for pions, kaons, and $p/\bar{p}$ (top to bottom, model represented by lines) are compared to PHENIX data [45]. Positive (negative) species are represented by circles (squares).

energy density from the boundaries of the two phases peaked at a value of $s/2\pi$. Elliptic flow, analyses of which are inherently precluded with the model used here due to an assumption of azimuthal symmetry, needs to be fit with the same parameters. More detailed aspects of femtoscopic data also need to be matched, such as radii with respect to the reaction plane [40], correlations of other species, especially nonidentical particles [41,42], and non-Gaussian features of the source function [43]. Even if all these data are reproduced, it does not fully validate the model. That would require an ambitious statistical analysis of the set of model parameters and assumptions, similar to [44]. Although these goals require significant effort in the coming years, the current analysis has eliminated any puzzle about femtoscopy for the time being, as the experimental radii appear to be satisfactorily described within a rather standard theoretical picture of RHIC collision dynamics.

[1] K. Adcox *et al.* (PHENIX Collaboration), Nucl. Phys. **A757**, 184 (2005).
[2] J. Adams *et al.* (STAR Collaboration), Nucl. Phys. **A757**, 102 (2005).
[3] U. W. Heinz and P. F. Kolb, arXiv:hep-ph/0204061.
[4] D. Teaney, J. Lauret, and E. V. Shuryak, arXiv:nucl-th/0110037.
[5] S. Soff, S. A. Bass, and A. Dumitru, Phys. Rev. Lett. **86**, 3981 (2001).
[6] T. Hirano and K. Tsuda, Nucl. Phys. **A715**, 821 (2003).
[7] M. A. Lisa, S. Pratt, R. Soltz, and U. Wiedemann, Annu. Rev. Nucl. Part. Sci. **55**, 357 (2005).
[8] R. Hanbury Brown and R. Q. Twiss, Nature (London) **178**, 1046 (1956).
[9] H. Petersen, J. Steinheimer, Q. Li, G. Burau, and M. Bleicher, arXiv:0806.1805.
[10] Q. Li, M. Bleicher, and H. Stocker, Phys. Lett. B **663**, 395 (2008).
[11] T. J. Humanic, AIP Conf. Proc. **828**, 625 (2006).
[12] Z.-W. Lin, C. M. Ko, and S. Pal, Phys. Rev. Lett. **89**, 152301 (2002).
[13] S. Pratt and J. Vredevoogd, Phys. Rev. C **78**, 054906 (2008).
[14] W. Broniowski, M. Chojnacki, W. Florkowski, and A. Kisiel, Phys. Rev. Lett. **101**, 022301 (2008).
[15] S. E. Koonin, Phys. Lett. B **70**, 43 (1977).
[16] J. Adams *et al.* (STAR Collaboration), Phys. Rev. C **71**, 044906 (2005).
[17] M. G. Bowler, Phys. Lett. B **270**, 69 (1991).
[18] Y. Sinyukov, R. Lednicky, S. V. Akkelin, J. Pluta, and B. Erazmus, Phys. Lett. B **432**, 248 (1998).
[19] M. Gyulassy, Y. M. Sinyukov, I. Karpenko, and A. V. Nazarenko, Braz. J. Phys. **37**, 1031 (2007).
[20] P. F. Kolb and R. Rapp, Phys. Rev. C **67**, 044903 (2003).
[21] U. W. Heinz and S. M. H. Wong, Phys. Rev. C **66**, 014907 (2002).
[22] A. Krasnitz, Y. Nara, and R. Venugopalan, Phys. Lett. B **554**, 21 (2003).
[23] J. Vredevoogd and S. Pratt, Phys. Rev. C **79**, 044915 (2009).
[24] S. Pratt, Phys. Rev. D **33**, 1314 (1986).
[25] D. H. Rischke and M. Gyulassy, Nucl. Phys. **A608**, 479 (1996).
[26] Y. Hama, R. P. G. Andrade, F. Grassi, O. Socolowski, Jr., T. Kodama, B. Tavares, and S. S. Padula, Nucl. Phys. **A774**, 169 (2006).
[27] D. Teaney, Phys. Rev. C **68**, 034913 (2003).
[28] P. Romatschke and U. Romatschke, Phys. Rev. Lett. **99**, 172301 (2007).
[29] P. Kovtun, D. T. Son, and A. O. Starinets, Phys. Rev. Lett. **94**, 111601 (2005).
[30] K. Paech and S. Pratt, Phys. Rev. C **74**, 014901 (2006).
[31] F. Karsch, D. Kharzeev, and K. Tuchin, Phys. Lett. B **663**, 217 (2008).
[32] P. F. Kolb, J. Sollfrank, and U. W. Heinz, Phys. Rev. C **62**, 054909 (2000).
[33] H.-J. Drescher, A. Dumitru, C. Gombeaud, and J.-Y. Ollitrault, Phys. Rev. C **76**, 024905 (2007).
[34] S. Pratt, Phys. Rev. C **75**, 024907 (2007).
[35] J. G. Cramer, G. A. Miller, J. M. S. Wu, and J.-H. Yoon, Phys. Rev. Lett. **94**, 102302 (2005).
[36] S. Pratt, AIP Conf. Proc. **828**, 213 (2006).
[37] F. Retiere and M. A. Lisa, Phys. Rev. C **70**, 044907 (2004).
[38] A. Kisiel, W. Florkowski, and W. Broniowski, Phys. Rev. C **73**, 064902 (2006).
[39] S. Pratt and J. Murray, Phys. Rev. C **57**, 1907 (1998).
[40] J. Adams *et al.* (STAR Collaboration), Phys. Rev. Lett. **93**, 012301 (2004).
[41] A. Kisiel (STAR Collaboration), J. Phys. G **30**, S1059 (2004).
[42] J. Adams *et al.* (STAR Collaboration), Phys. Rev. Lett. **91**, 262302 (2003).
[43] S. Y. Panitkin *et al.* (E895 Collaboration), Phys. Rev. Lett. **87**, 112304 (2001).
[44] S. Habib, K. Heitmann, D. Higdon, C. Nakhleh, and B. Williams, Phys. Rev. D **76**, 083503 (2007).
[45] S. S. Adler *et al.*, Phys. Rev. C **69**, 034909 (2004).